Published in final edited form as:
J Immunol. 2010 February 15; 184(4): 1821–1828. doi:10.4049/jimmunol.0902869.

Dynamic Equilibrium of B7-1 Dimers and Monomers Differentially Affects Immunological Synapse Formation and T Cell Activation in Response to TCR/CD28 Stimulation

Sumeena Bhatia[*], **Kristine Sun**[*], **Steven C. Almo**[†,‡], **Stanley G. Nathenson**[§,¶], and **Richard J. Hodes**[*]

[*]Experimental Immunology Branch, National Cancer Institute, National Institutes of Health, Bethesda, MD 20892

[†]Department of Biochemistry, Albert Einstein College of Medicine, Bronx, NY 10461

[‡]Department of Physiology and Biophysics, Albert Einstein College of Medicine, Bronx, NY 10461

[§]Department of Microbiology and Immunology, Albert Einstein College of Medicine, Bronx, NY 10461

[¶]Department of Cell Biology, Albert Einstein College of Medicine, Bronx, NY 10461

Abstract

Under steady-state conditions, B7-1 is present as a mixed population of noncovalent dimers and monomers on the cell surface. In this study, we examined the physiological significance of this unique dimer–monomer equilibrium state of B7-1. We demonstrate that altering B7-1 to create a uniformly covalent dimeric state results in enhanced CD28-mediated formation of T cell–APC conjugates. The enhanced T cell–APC conjugate formation correlates with persistent concentration of signaling molecules PKC-u and lck at the immunological synapse. In contrast, T cell acquisition of B7-1 from APCs, an event that occurs as a consequence of CD28 engagement with B7-1/B7-2 and is thought to play a role in the dissociation of T cell–APC conjugates, is highly reduced when B7-1 is present in the covalently dimeric state. The ability of covalently dimeric and wild type B7-1 to costimulate Ag-specific T cell proliferation was also assessed. In contrast to the enhanced ability of dimeric B7-1 to support conjugate formation and early parameters of T cell signaling, sensitivity to competitive inhibition by soluble CTLA-4–Ig indicated that the covalent dimeric form of B7-1 is less efficient in costimulating T cell proliferation. These findings suggest a novel model in which optimal T cell costimulatory function of B7-1 requires high-avidity CD28 engagement by dimeric B7-1, followed by dissociation of these non-covalent B7-1 dimers, facilitating downregulation of CD28 and internalization of B7-1. These events regulate signaling through TCR/CD28 to maximize T cell activation to proliferation.

Address correspondence and reprint requests to Dr. Richard J. Hodes, Experimental Immunology Branch, Center for Cancer Research, National Cancer Institute, National Institutes of Health, 10 Center Drive, Building 10, Room 4B36, Bethesda, MD 20892. hodesr@31.nia.nih.gov.

Disclosures

The authors have no financial conflicts of interest.

Interaction of B7-1 and B7-2 with the T cell costimulatory receptor CD28 augments T cell activation, resulting in IL-2 production, proliferation, and differentiation, whereas interaction of B7-1 and B7-2 with the T cell inhibitory receptor CTLA-4 results in termination of T cell response and induces T cell anergy (1, 2). B7-1 and B7-2 are structurally homologous molecules and share the receptors CD28 and CTLA-4, yet they exhibit several distinct features. B7-2 is constitutively expressed on APCs and is rapidly upregulated upon activation with maximal expression at 48 h, whereas B7-1 is slowly induced upon activation of APCs, and its level of expression is stable for 48–96 h (3, 4). In addition, biochemical analyses demonstrated that B7-2 binds to its receptors with ~10–100-fold lower affinity than B7-1 (5). B7-1 binds CTLA-4 and CD28 with equilibrium K_d of 0.2 and 0.4 μM, whereas the K_d values of B7-2 are 2.6 and 20 μM for CTLA-4 and CD28, respectively (6). Imaging of the recruitment and accumulation of B7-1/B7-2 and CD28/CTLA-4 at the immunological synapse (IS) suggested that B7-1 and B7-2 differ in their prefer ential pairing with CD28 and CTLA-4 (7). Although B7-1 and B7-2 seem to have overlapping functions, numerous reports suggested distinct immunological effects (8–13). It is not clearly understood whether these disparities arise from differences in the expression of B7-1/B7-2 on different cell types, from differences in kinetics of expression, or reflect intrinsic functional differences between these costimulatory molecules.

Structural studies revealed differences between B7-1 and B7-2, which may be important in mediating the functions of these costimulatory molecules. Analysis of purified B7 molecules showed that B7-1 crystallizes as a dimer, in contrast to B7-2, which is detected as a monomer in the crystalline state (14, 15). Our recent studies using cell-based photobleaching-fluorescence resonance energy transfer demonstrated that B7-1 and B7-2 also have distinct oligomeric states on the cell surface that may contribute to fundamental mechanisms of T cell activation. Under steady-state conditions, B7-2 is expressed as a monomer on the cell surface, whereas B7-1 is expressed as a mixed population composed predominantly of noncovalent dimers and a lower proportion of monomers (16). The monomeric versus dimeric state of B7-2 and B7-1, respectively, may allow for the formation of qualitatively different complexes with CD28 or CTLA-4 on the cell surface and the assembly of different macromolecular signaling complexes in the IS (17).

Although B7-1 is present as a mixture of noncovalent dimers and monomers on the cell surface, the functional significance of this mixed population is not known. In the current study, we examined the role of the B7-1 monomer–dimer equilibrium in T cell costimulation by generating obligate covalent B7-1 dimers and characterizing the function of these molecules in the interaction with and activation of T cells. Our observations suggest that the B7-1 monomer–dimer equilibrium is important for modulating signaling through the TCR/CD28 pathways and the regulation of T cell activation.

Materials and Methods

Mice

DO11.10 TCR transgenic (Tg) mice (18) were a gift from Dr. David Segal (National Cancer Institute, National Institutes of Health). DO11.10.B7-$1^{-/-}$ B7-2-DKO mice were generated by breeding DO11.10 TCR Tg mice to B7-$1^{-/-}$B7-2-DKO mice. DO11.10 TCR Tg mice

were bred to CD28KO mice (The Jackson Laboratory, Bar Harbor, ME) to obtain DO11.10 $CD28^{-/-}$ mice. All mice were maintained on a BALB/c background. Sixto eight-week-old mice were used for all experiments. Mice were bred, maintained, and housed at Bioqual (Rockville, MD). All animal experiments were approved by the National Cancer Institute Animal Care and Use Committee.

Cell preparation

$CHO\text{-}IA^d$ cells were a generous gift of Dr. Arlene Sharpe (Harvard University, Boston, MA). Stable transfectants of $CHO\text{-}IA^d$ cells were prepared by transfecting with cDNA encoding the wild type (WT) or mutant B7-1 using Lipofectamine (Invitrogen, Carlsbad, CA). Zeocin-resistant stable clones were obtained by repeated rounds of subcloning and sorting. Stable clones expressing equivalent levels of WT or mutant B7-1 were used in all experiments.

T cells were isolated from spleen using MACS CD4 T cell isolation kit (Miltenyi Biotec, Auburn, CA). Negatively selected T cells were 95–98% pure, as determined by flow cytometry.

Flow cytometry

Expression of WT or mutant B7-1 molecules on CHO cells was determined using APC-conjugated anti–B7-1 MAb 16.10A1 (eBioscience, San Diego, CA). For binding to CD28 or CTLA-4, CHO-IAd cells expressing WT or mutant B7-1 were incubated with fusion proteins CD28Ig or CTLA-4Ig (R&D Systems, Minneapolis, MN), followed by detection with Cy5-conjugated anti-human IgG (Jackson ImmunoResearch Laboratories, West Grove, PA).

Fluorescent labeling of cells

$CHO\text{-}IA^d$ (untransfected or stably transfected with B7-1) were labeled with chloromethyl-benzoyl-amino-tetramethylrhodamine CMTMR (Molecular Probes, Eugene, OR), and isolated DO11.10 CD4 T cells were labeled with CFSE (Molecular Probes), per the manufacturer's protocol. Briefly, peptide-pulsed $CHO\text{-}IA^d$ cells were labeled with 1 μM CMTMR in serum-free RPMI 1640 medium for 30 min at 37°C. Cells were then washed, re-suspended in complete medium, and incubated for an additional 30 min at 37°C. Subsequently, cells were washed twice with PBS prior to use in T cell–APC conjugate assays. Purified CD4 T cells were labeled with 5 μM CFSE at room temperature (RT) for 5 min, washed three times with PBS containing 5% FCS, and finally resuspended in complete medium.

Conjugate assay and fluorescence microscopy

Four to 8×10^5 CMTMR-labeled $CHO\text{-}IA^d$ cells, prepulsed with titrated concentrations of OVA peptide, were mixed with equal numbers of CFSE-labeled T cells for 2–3 h at 37°C. The cells were briefly vortexed before flow cytometry.

Peptide-pulsed $CHO\text{-}IA^d$ cells were mixed with equal numbers of purified DO11.10 CD4 T cells for 2–3 h at 37°C. Then the cells were adhered to poly-l-lysine–coated glass cover slips

for 5 min at RT, washed with PBS, and fixed with 4% paraformaldehyde for 20 min at RT. After washing, the cells were permeabilized with 0.1% Triton X-100 in PBS for 3–5 min. Cells were washed again with PBS, preincubated with PBS containing 1% BSA for 20–30 min at RT, and stained with the following Abs: anti–CD4-APC (Southern Biotechnology Associates, Birmingham, AL), anti–B7-1-FITC (BD Biosciences, San Jose, CA), anti–protein kinase C (PKC)-θ (C-18; Santa Cruz Biotechnology, Santa Cruz, CA), or anti-lck (3A5; Santa Cruz Biotechnology) for 1 h at RT. PKC-θ and lck were detected by using anti-rabbit IgG-Alexa Fluor 546 and anti-mouse IgG2-FITC, respectively, as secondary Abs for 1 h at RT. The cells were washed extensively, and the cover slips were mounted on slides using ProLong Anti-Fade mounting medium (Molecular Probes). Cells were imaged at a magnification of 2× on a Zeiss LSM 510 Meta laser-scanning confocal microscope(Carl Zeiss Microimaging, Thornwood, NY) using an ×63/1.4 oil objective lens.

For B7-1 internalization, midoptical slices of T cell–APC conjugates were acquired. T cells in T cell–APC conjugates that showed fluorescence in the B7-1 channel greater than the threshold value based on the B7-1 channel in T cells only were scored positive for acquisition of B7-1. Images were processed and analyzed using ImageJ (http://rsbweb.nih.gov/ij/; National Institutes of Health, Bethesda, MD).

For PKC-θ and lck, image stacks consisting of eight to 11 planes spaced by 1 μm were collected. The ratio of fluorescence intensity at the IS to the fluorescence intensity at the distal membrane was used to calculate fold enrichment of the signaling molecules at the IS. T cell–APC conjugates that showed >2-fold enrichment of PKC-θ in the IS were scored as positive events. Fifty to 70 conjugates were imaged per group per experiment. All images were processed using LSM 5 Image Examiner. 2.5D view, and xz/yz reconstruction was done on z-stacks of images using LSM 5 Image Examiner(Carl Zeiss Microimaging).

T cell proliferation assay

Stable transfectants of CHO-IA^d cells expressing various mutants of B7-1 were treated with 50 μg/ml mitomycin C (Fisher, Pittsburgh, PA) overnight at 37°C. Cells were harvested using 2 mM EDTA and washed extensively prior to their use as APCs. One × 10^5 DO.11 CD4$^+$ T cells were stimulated with a titrated concentration of OVA peptide (323–339) in the presence of 5 × 10^4 mitomycin C-treated CHO-IA^d transfectants in 96-well plates for 48 h. CTLA-4–Ig was added as indicated. One μCi [^{3}H]thymidine was added per well for an additional 16 h. The [^{3}H]thymidine incorporation was determined using a scintillation counter.

Results

WT B7-1 and covalently linked obligate dimeric B7-1 are equivalent in their binding to CD28 and CTLA-4

To study the role of B7-1 dimer–monomer equilibrium in T cell costimulation, we generated stable transfectants of CHO-IA^d cells as a model of APCs expressing the WT B7-1 (B7-1), B7-1 engineered with a short 8-aa residue linker sequence containing a cysteine (B7-1–cysteine), or B7-1 containing the same linker sequence without the cysteine (B7-1–control)

(Fig 1*A*). Our unpublished observations showed that, similar to WT B7-1, B7-1– control exists on the cell surface as a mixed population of monomers and dimers. The presence of cysteine in the extracellular stalk of B7-1 results in the formation of disulfide-linked covalent B7-1 dimers, thus switching the mixed distribution of B7-1 to a uniform dimeric state on the cell surface (16). Stable clones expressing equivalent levels of WT, B7-1– control, or B7-1–cysteine were selected for subsequent experiments (Fig. 1*B*). Levels of B7-1 expression on these transfectants were comparable to that of in vitro-activated splenic dendritic cells (Fig. 1*B*, *right panel*). As shown in Fig. 1*C*, at titrated concentrations of CD28-Ig or CTLA-4Ig, the covalently linked dimeric form of B7-1 binds to these receptors at levels comparable to those of WT or control B7-1, suggesting that altering the oligomeric state of B7-1 does not affect its receptor-binding property.

Covalently dimeric state of B7-1 increases CD28-mediated adhesion of APCs to T cells

The interaction of B7-1 or B7-2 on APCs with CD28 on T cells mediates enhanced adhesion of APCs and T cells (19). To study the relationship of the B7-1 oligomeric state to CD28-dependent T cell adhesion, we used stable transfectants of CHO-IA^d as APCs in experiments assessing B7-1 function in T cell–APC interactions. CMTMR-labeled CHO-IA^d APCs expressing WT B7-1, B7-1– control, or B7-1–cysteine were mixed with CFSE-labeled DO11.10 TCR Tg CD4$^+$ T cells in the presence of various concentrations of the OVA peptide. CMTMR$^+$CFSE$^+$ double-positive events were scored as T cell–APC conjugates. The expression of WT B7-1 (Fig. 2*A*, *second row*) or B7-1–control (Fig. 2A, third row) on CHO-IA^d cells resulted in an increase in Ag-dependent T cell–APC conjugates compared with untransfected CHO-IA^d cells (Fig. 2*A*, *top row*). However, when the CHO-IA^d cells expressed B7-1–cysteine (Fig. 2*A*, *bottom row*), there was a greater increase in the formation of conjugates relative to WT B7-1 or control B7-1. Quantification of DO11.10 TCR Tg CD4$^+$ T cell conjugates with CHO-IA^d cells expressing WT B7-1, B7-1–control, or B7-1–cysteine indicated that B7-1–cysteine results in the formation of a significantly greater number of conjugates in a peptide-dependent manner (Fig. 2*B*). T cells from CD28-deficient mice generated comparable and very low frequencies (<5%) of T cell–APC conjugates with untransfected or B7-1–expressing CHO-IA^d cells, indicating that enhancement of T cell–APC conjugate formation in the presence of B7-1 is CD28-dependent (Supplemental Fig. 1). Thus, CD28-dependent interaction with the obligate dimeric B7-1–cysteine results in enhanced formation of Ag-dependent T cell–APC conjugates.

Covalently dimeric state of B7-1 results in higher and persistent localization of lck and PKC-θ at the IS

Clustering of cell surface molecules, including TCR, CD28, and LFA-1, in the T cell–APC interface occurs following formation of conjugates between T cells and APCs (20–22). Moreover, intracellular signaling molecules, such as PKC-θ, lck, and ZAP-70, are also concentrated at the IS and direct the initiation of TCR signaling (20, 23, 24). To determine whether the dimeric state of B7-1 affects formation of productive ISs, we used immunofluorescence and confocal imaging to follow the kinetics of clustering of signaling molecules PKC-θ and lck at the T cell–APC interface. DO11.10 Tg T cells and peptide-pulsed CHO-IA^d cells expressing the B7-1–control or B7-1–cysteine were mixed for various periods of time (2, 7, and 20 min); the resulting conjugates were fixed and stained for

intracellular PKC-θ and lck. Fig. 3A shows representative images of enrichment and localization of PKC-θ (*upper left panel*) and lck (*upper right panel*) in the IS. Translocation of PKC-θ and enrichment of lck to the IS were observed as early as 2 min after T cell–APC conjugate formation. Quantification of the proportion of conjugates that showed >2-fold enrichment of PKC-θ in the IS revealed significant differences between B7-1–control and B7-1–cysteine. Within 2 min of T cell–APC conjugate formation in the presence of B7-1–cysteine, ~60–70% of T cell conjugates were detected with strong PKC-θ concentration (>2-fold) at the IS (Fig. 3*B*, *left graph*), which was significantly greater than observed in the presence of B7-1–control (40%) and was substantially greater than observed in the few conjugates that were formed with APCs lacking B7-1 expression. Moreover, B7-1–cysteine-expressing APCs sustained high concentrations of PKC-θ at the IS for as long as 20 min, whereas in the presence of B7-1–control, control, the percentages of T cell conjugates exhibiting a concentration of PKC-θ at the IS were not different from those in B7-1–negative APCs. Quantification of the degree of concentration of lck in the IS revealed that at 2 min, 70% of T cell conjugates showed strong accumulation (>1.5-fold) in the presence of B7-1– cysteine, whereas only 46% of T cells showed strong accumulation of lck in the presence of B7-1–control (Fig. 3*B*, *right graph*). A similar pattern was observed at 7 min. By 20 min, lck recruitment to the IS had decreased and was equivalent in the absence or presence of B7-1–control or B7-1–cysteine (data not shown). Taken together, these data suggest that the perturbation of the B7-1 monomer–dimer equilibrium via incorporation of a covalent disulfide bond, resulting in an exclusively dimeric population, leads to increased and persistent concentration of intracellular signaling molecules PKC-θ and lck at the IS.

It was reported that CD28 is required for the segregation of PKC-θ within the mature IS (25). To further analyze the role of the dimeric state of B7-1 in the segregation of signaling/accessory molecules in the IS, we stained T cell–APC conjugates for PKC-θ and LFA-1. Fig. 3*C* (*left panel*) shows a representative image of a T cell–APC conjugate, showing the segregation of PKC-θ and LFA-1 in the IS when T cells from DO11.10 mice were used. 2.5D plots clearly show the exclusion of LFA-1 from the center of IS where PKC-θ is found to be enriched. xz reconstruction of the IS also distinctly shows PKC-θ in the center, surrounded by LFA-1, a hallmark of a mature IS (21). Quantification of T cells with segregated mature ISs revealed a considerable difference between B7-1–negative APCs and APCs expressing B7-1–control (Fig. 3D). Although B7-1–negative and B7-1–control APCs did not differ in their ability to induce translocation of PKC-θ to the IS (Fig. 3*B*, *left graph*), the segregation of PKC-θ within the IS was markedly enhanced in the presence of B7-1–CD28 interaction. The requirement for B7-1–CD28 interaction in the formation of the mature IS was further reinforced using T cells from CD28-deficient mice, wherein no clear segregation of PKC-θ and LFA-1 within the IS was observed (Fig. 3*D*, Supplemental Fig. 2). B7-1– control and B7-1–cysteine did not differ in their ability to induce the segregation of molecules within the IS, suggesting that the dimeric state of B7-1 plays a significant role in the enrichment of PKC-θ and lck to the IS (Fig. 3B) but a limited role in the segregation of these molecules within the IS (Fig. 3D).

Reduced acquisition of covalently linked dimeric B7-1 by T cells

It was demonstrated that, during T cell–APC interaction, TCR and CD28 expressed on T cells mediate the cell surface acquisition and internalization of APC-derived molecules, notably peptide-MHC and B7-1/B7-2 (26–29). Moreover, there is a close correlation between CD28 downregulation and B7-1 acquisition by T cells, suggesting that B7-1 engagement of CD28 leads to internalization of B7-1–CD28 complexes (26). These events may contribute to the dissociation of T cell–APC conjugates and termination of T cell activation. Given our observations that covalently linked dimeric B7-1 resulted in increased T cell–APC conjugate formation and enhanced concentration of signaling molecules at the IS, we assessed whether T cell acquisition of B7-1, a possible surrogate for internalization of CD28, is influenced by the cell surface oligomeric state of B7-1. Although the low level of expression of endogenous CD28 on T cells presents an obstacle to following its intracellular trafficking by direct imaging techniques, B7-1 acquired by T cells is easily detected (26). Hence, we used confocal imaging to visualize B7-1 in T cells that had been acquired from APCs upon formation of conjugates with APCs expressing B7-1 or B7-1–cysteine. Fig. 4*A* shows representative images of the acquisition of WT B7-1 (*left panel*) or B7-1–cysteine (*right panel*) by WT (*first and third rows*) or CD28-deficient DO11.10 TCR Tg T cells (*second and fourth rows*) at indicated time points. T cells used in these experiments were deficient in endogenous B7-1 and B7-2, so that any fluorescence signal (intracellular or cell surface associated) observed for B7-1 in T cells must represent B7-1 acquired from the APCs. Quantification of the acquisition of B7-1–control or B7-1–cysteine at 3 h in the presence or absence of peptide revealed significant differences. In the absence of peptide, ~20% of T cells in conjugates showed acquisition of B7-1 when APCs expressed B7-1–control or B7-1–cysteine. However, in the presence of OVA peptide, B7-1 was acquired by 60–70% of T cells in conjugates with APCs expressing B7-1–control, whereas the frequency of T cells acquiring B7-1–cysteine was not increased over background levels observed in the absence of peptide (Fig. 4*B*, *left graph*). Quantification of total B7-1 fluorescence also revealed that a greater amount of B7-1–control was acquired per T cell in the presence of peptide compared with B7-1–cysteine (Fig. 4*B*, *right graph*). Additional experiments were carried out comparing the acquisition of B7-1 in conjugates with WT or $CD28^{-/-}$ DO11.10 TCR Tg T cells. Acquisition of B7-1 by T cells was observed as early as 30 min after T cell–APC conjugate formation (Fig. 4*C*, *left graph*), and it increased by 3 h when WT B7-1–expressing APCs were used (Fig. 4C, *right graph*). However, substantially less B7-1–cysteine acquisition was observed at both time points. B7-1 acquisition was almost completely absent when T cells from $CD28^{-/-}$ DO11.10 TCR Tg mice were used (Fig 4C), demonstrating that B7-1 acquisition by T cells was CD28 dependent. Thus, B7-1–cysteine failed to mediate Ag-dependent, CD28-mediated acquisition of B7-1 by T cells during T cell–APC interaction, suggesting that CD28 internalization is prevented by obligate dimerization of B7-1.

Covalently dimeric B7-1 is less efficient in costimulation for T cell proliferation

Altering the strength and duration of TCR signal and costimulation were demonstrated to have profound and complex effects on T cell activation. For example, sustained interactions between TCR and peptide-MHC were shown to paradoxically impair T cell activation (30,

31). On the other hand, strong costimulatory signals can convert a weak agonist peptide to a strong agonist peptide (32). Given our observation that covalent dimerization of B7-1 can result in enhanced T cell–APC conjugate formation and the concentration of proximal T cell signaling molecules at the IS, we assessed its effect on T cell proliferation. Purified $CD4^+$ T cells from DO11.10 ($B7\text{-}1^{-/-}$ $B7\text{-}2^{-/-}$ DKO) TCR Tg mice were stimulated with varying concentrations of OVA peptide in the presence of B7-negative CHO-IA^d cells or CHO-IA^d cells expressing WT B7-1, B7-1– control, or B7-1–cysteine. WT, B7-1–control, and B7-1–cysteine-expressing APCs induced equivalent levels of T cell proliferation (Fig. 5*A*, *top graph*). The B7-1–mediated costimulatory effect on T cell proliferation was completely lost when DO11.10 TCR Tg T cells were derived from CD28-deficient mice, indicating that proliferation is dependent on B7-1–CD28 interaction (Fig. 5*A*, bottom graph). The level of expression of B7-1 on the transfected APCs used in these studies is comparable to that expressed on highly in vitro-activated dendritic cells (Fig. 1*B*), and it remained possible that these high levels of expression might obscure differences between B7-1 molecular species that would be manifest at limiting and potentially physiologic levels of B7-1. To provide a sensitive, quantitative measure of the efficiency of costimulation provided under these conditions, we measured the susceptibility to inhibition of proliferation by soluble CTLA-4–Ig. At high concentrations of CTLA-4–Ig (0.25 μg/ml), an 80–90% inhibition in T cell proliferation response was observed, irrespective of the form of B7-1 that was expressed on CHO-IA^d cells (Fig. 5*B*, *top graph*). However, at low concentrations of CTLA-4–Ig (0.025 μg/ml), T cell proliferative responses to WT B7-1 or B7-1–control were only minimally inhibited (5–20%), whereas T cell responses to B7-1– cysteine showed significantly greater inhibition (50–60%) (Fig. 5*B*, *bottom graph*). Thus, under conditions of limiting B7-1, as achieved by CTLA-4–Ig competition, B7-1–cysteine is substantially less efficient than B7-1–control in costimulating T cell proliferation.

Discussion

Previous studies demonstrated that cell surface B7-1 exists as a mixture of monomer and dimer in apparent equilibrium. In the current study, the functional role of the physiologic B7-1 monomer–dimer state in T cell activation was examined by altering this equilibrium through the generation of covalent dimers of B7-1. We compared the costimulatory properties of the covalently linked obligate dimeric form of B7-1 with that of WT B7-1 by examining the effects on early and late events of T cell activation.

We found that covalently linked dimers of B7-1 mediate strong and persistent early events in T cell–APC interaction and T cell activation. Covalent dimeric B7-1–cysteine resulted in frequencies of CD28-dependent T cell–APC conjugates higher than those mediated by WT control B7-1. Moreover, T cell–APC conjugates formed with covalent dimeric B7-1–cysteine, but not with WT control B7-1, showed enhanced and sustained accumulation of signaling molecules PKC-θ and lck at the IS. PKC-θ was shown to specifically localize to the central region of the IS and to persist for a prolonged period of time, from 30 min to as long as 4 h (25). lck is also rapidly recruited to the T cell–APC interface, although its clustering in the IS is relatively short lived, occurring as early as 3 min, with maximal clustering at 7 min and much reduced levels by 23 min (20). Signaling through CD28 was shown to be important for sustained phosphorylation of lck at the IS (24). Consistent with

these reports, costimulation by B7-1–cysteine resulted in increased and sustained localization of PKC-θ at the IS, as well as increased rapid and strong recruitment of lck relative to that observed for B7-1–control. B7-1–CD28 interaction-dependent segregation of PKC-θ/LFA-1 within the IS, a hallmark of mature IS, was observed; however, the ability to induce this segregation was not affected by altering the cell surface oligomeric state of B7-1 and was equivalent for B7-1–control and B7-1–cysteine. Therefore, these data suggest differential effects of the B7-1 dimer–monomer equilibrium on the accumulation of signaling molecules at the IS and their segregation within the IS.

Because the strength and duration of TCR and costimulatory signals can have significant and complex effects on the final outcome of T cell activation (30–32), the efficiency of covalently linked dimeric B7-1 in the costimulation of T cell proliferation was evaluated under conditions in which the strength of the costimulatory signal could be modulated using competitive inhibition by soluble CTLA-4–Ig. In the presence of a limiting concentration of CTLA-4–Ig, T cell proliferation induced by covalently linked B7-1 was significantly less than that induced by costimulation with WT B7-1 or B7-1–control. Thus, the covalent dimeric form of B7-1 was capable of initiating strong and persistent early signaling; however, it was less effective in providing costimulation for T cell proliferation. A similar divergence of strong TCR and/or costimulatory signal, yet reduced T cell activation, was reported for CD8 T cells (31, 33). Decreasing the dissociation of peptide-MHC from its TCR, and thus augmenting the $t_{1/2}$ of peptide-MHC–TCR interaction, was shown to reduce T cell activation, as measured by cytokine production and the induction of cytolytic activity (31). In another experimental system, enhanced costimulation by B7-1 led to reduced CD8 T cell proliferation and cytokine production (33).

The acquisition of peptide-MHC and costimulatory ligands, such as B7-1, was shown to occur rapidly during T cell–APC interaction (26, 27), and internalization of CD28 by T cells was shown to occur concomitantly with B7-1 absorption (26). Of the surface CD28 that is internalized, almost half is targeted to lysosomes for degradation, whereas the remaining is recycled back to the T cell membrane (34). Although the biological significance of this CD28 trafficking in not clear, it is possible that the absorption of key stimulatory molecules, such as peptide-MHC and B7-1, and internalization of CD28 may serve as one of several mechanisms to dissociate T cell–APC conjugates and that this may be required for serial triggering of multiple T cells in the presence of highly limited ligand (35). The removal of peptide-MHC and B7-1 from the T cell–APC synapse and the dissociation of T cell–APC conjugates may also be required to regulate the strength and duration of the signals delivered to the T cells through TCR and CD28 and, thus, to regulate T activation. Our data are consistent with the hypothesis that the removal of peptide-MHC and B7-1 from the IS and the dissociation of receptors from ligands may be a mechanism to modulate signaling in T cells. The covalent dimeric form of B7-1, which can form more stable T cell–APC conjugates and deliver strong and persistent signal to T cells, is poorly acquired by T cells. Because there is a close correlation between B7-1 absorption and CD28 internalization (26, 27), it is likely that increased CD28 retained at the T cell surface in the IS may continue to transduce persistent signal in T cells, with consequences for downstream events and T cell response.

Our observations suggest a model in which the cell surface oligomeric state of B7-1 contributes to the regulation of T cell activation. The optimal costimulatory function of B7-1 may require the efficient high-avidity initial engagement of CD28 by dimers of B7-1, followed by dissociation to monomer, which facilitates events, such as the internalization of CD28 and the acquisition of B7-1 by T cells (Fig. 6*A*). This process ensures an optimum dwell time of T cell–APC costimulatory interaction and cell contact, thereby regulating signal transduction to achieve effective T cell activation. However, when the noncovalent dimers of B7-1 are replaced by covalently linked obligate dimers, B7-1 is unable to undergo dissociation after binding to CD28 (Fig. 6*B*). Consequently, B7-1 and CD28 are trapped at the T cell–APC interface, resulting in persistent signaling, as manifested by the persistent accumulation of PKC-θ and lck at the T cell–APC interface. It was shown that although CD4 aids in recruitment of lck to the T cell– APC interface, CD28 is important for sustained lck activation (24). Thus, the persistent expression of CD28 may lead to sustained accumulation of lck at the IS, as is observed with the covalently linked dimeric form of B7-1. Hence, the dissociation of noncovalent dimers of B7-1 may play an important role in maintaining the optimum dynamic expression of CD28 on T cell surface and in regulating the strength and kinetics of CD28-mediated signal transduction optimal for activating T cell proliferation and function.

Acknowledgments

We thank K. Hathcock and A. Singer for the critical reading of the manuscript; G. Sanchez-Howard and the staff at Bioqual for excellent animal care and husbandry; S. Sharrow, T. Adams, and L. Granger for flow cytometry; and M. Kruhlak for imaging.

This work was supported by the Intramural Research Program of the National Cancer Institute, National Institutes of Health.

Abbreviations used in this paper

CMTMR	chloromethyl-benzoyl-amino-tetrame thylrhodamine
IS	immunological synapse
ns	not significant
PKC	protein kinase C
RT	room temperature
Tg	transgenic
WT	wild type

References

1. Greenwald RJ, Freeman GJ, Sharpe AH. The B7 family revisited. Annu. Rev. Immunol. 2005; 23:515–548. [PubMed: 15771580]
2. Keir ME, Sharpe AH. The B7/CD28 costimulatory family in autoimmunity. Immunol. Rev. 2005; 204:128–143. [PubMed: 15790355]
3. Hathcock KS, Laszlo G, Pucillo C, Linsley P, Hodes RJ. Comparative analysis of B7-1 and B7-2 costimulatory ligands: expression and function. J. Exp. Med. 1994; 180:631–640. [PubMed: 7519245]

4. Inaba K, Witmer-Pack M, Inaba M, Hathcock KS, Sakuta H, Azuma M, Yagita H, Okumura K, Linsley PS, Ikehara S, et al. The tissue distribution of the B7-2 costimulator in mice: abundant expression on dendritic cells in situ and during maturation in vitro. J. Exp. Med. 1994; 180:1849–1860. [PubMed: 7525841]
5. Collins AV, Brodie DW, Gilbert RJ, Iaboni A, Manso-Sancho R, Walse B, Stuart DI, van der Merwe PA, Davis SJ. The interaction properties of costimulatory molecules revisited. Immunity. 2002; 17:201–210. [PubMed: 12196291]
6. van der Merwe PA, Davis SJ. Molecular interactions mediating T cell antigen recognition. Annu. Rev. Immunol. 2003; 21:659–684. [PubMed: 12615890]
7. Pentcheva-Hoang T, Egen JG, Wojnoonski K, Allison JP. B7-1 and B7-2 selectively recruit CTLA-4 and CD28 to the immunological synapse. Immunity. 2004; 21:401–413. [PubMed: 15357951]
8. Freeman GJ, Boussiotis VA, Anumanthan A, Bernstein GM, Ke XY, Rennert PD, Gray GS, Gribben JG, Nadler LM. B7-1 and B7-2 do not deliver identical costimulatory signals, since B7-2 but not B7-1 preferentially costimulates the initial production of IL-4. Immunity. 1995; 2:523–532. [PubMed: 7538442]
9. Kuchroo VK, Das MP, Brown JA, Ranger AM, Zamvil SS, Sobel RA, Weiner HL, Nabavi N, Glimcher LH. B7-1 and B7-2 costimulatory molecules activate differentially the Th1/Th2 developmental pathways: application to autoimmune disease therapy. Cell. 1995; 80:707–718. [PubMed: 7534215]
10. Lenschow DJ, Ho SC, Sattar H, Rhee L, Gray G, Nabavi N, Herold KC, Bluestone JA. Differential effects of anti-B7-1 and anti-B7-2 monoclonal antibody treatment on the development of diabetes in the nonobese diabetic mouse. J. Exp. Med. 1995; 181:1145–1155. [PubMed: 7532678]
11. Jeannin P, Delneste Y, Lecoanet-Henchoz S, Gauchat JF, Ellis J, Bonnefoy JY. CD86 (B7-2) on human B cells. A functional role in proliferation and selective differentiation into IgE- and IgG4-producing cells. J. Biol. Chem. 1997; 272:15613–15619. [PubMed: 9188449]
12. Girvin AM, Dal Canto MC, Rhee L, Salomon B, Sharpe A, Bluestone JA, Miller SD. A critical role for B7/CD28 costimulation in experimental autoimmune encephalomyelitis: a comparative study using costimulatory molecule-deficient mice and monoclonal antibody blockade. J. Immunol. 2000; 164:136–143. [PubMed: 10605004]
13. Lumsden JM, Roberts JM, Harris NL, Peach RJ, Ronchese F. Differential requirement for CD80 and CD80/CD86-dependent costimulation in the lung immune response to an influenza virus infection. J. Immunol. 2000; 164:79–85. [PubMed: 10604996]
14. Ikemizu S, Gilbert RJ, Fennelly JA, Collins AV, Harlos K, Jones EY, Stuart DI, Davis SJ. Structure and dimerization of a soluble form of B7-1. Immunity. 2000; 12:51–60. [PubMed: 10661405]
15. Zhang X, Schwartz JC, Almo SC, Nathenson SG. Crystal structure of the receptor-binding domain of human B7-2: insights into organization and signaling. Proc. Natl. Acad. Sci. USA. 2003; 100:2586–2591. [PubMed: 12606712]
16. Bhatia S, Edidin M, Almo SC, Nathenson SG. Different cell surface oligomeric states of B7-1 and B7-2: implications for signaling. Proc. Natl. Acad. Sci. USA. 2005; 102:15569–15574. [PubMed: 16221763]
17. Bhatia S, Edidin M, Almo SC, Nathenson SG. B7-1 and B7-2: similar costimulatory ligands with different biochemical, oligomeric and signaling properties. Immunol. Lett. 2006; 104:70–75. [PubMed: 16413062]
18. Murphy KM, Heimberger AB, Loh DY. Induction by antigen of intrathymic apoptosis of CD4+CD8+TCRlo thymocytes in vivo. Science. 1990; 250:1720–1723. [PubMed: 2125367]
19. Linsley PS, Clark EA, Ledbetter JA. T-cell antigen CD28 mediates adhesion with B cells by interacting with activation antigen B7/BB-1. Proc. Natl. Acad. Sci. USA. 1990; 87:5031–5035. [PubMed: 2164219]
20. Freiberg BA, Kupfer H, Maslanik W, Delli J, Kappler J, Zaller DM, Kupfer A. Staging and resetting T cell activation in SMACs. Nat. Immunol. 2002; 3:911–917. [PubMed: 12244310]
21. Monks CR, Freiberg BA, Kupfer H, Sciaky N, Kupfer A. Three-dimensional segregation of supramolecular activation clusters in T cells. Nature. 1998; 395:82–86. [PubMed: 9738502]

22. Krummel MF, Davis MM. Dynamics of the immunological synapse: finding, establishing and solidifying a connection. Curr. Opin. Immunol. 2002; 14:66–74. [PubMed: 11790534]

23. Anton van der Merwe P, Davis SJ, Shaw AS, Dustin ML. Cytoskeletal polarization and redistribution of cell-surface molecules during T cell antigen recognition. Semin. Immunol. 2000; 12:5–21. [PubMed: 10723794]

24. Holdorf AD, Lee KH, Burack WR, Allen PM, Shaw AS. Regulation of Lck activity by CD4 and CD28 in the immunological synapse. Nat. Immunol. 2002; 3:259–264. [PubMed: 11828322]

25. Huang J, Lo PF, Zal T, Gascoigne NR, Smith BA, Levin SD, Grey HM. CD28 plays a critical role in the segregation of PKC theta within the immunologic synapse. Proc. Natl. Acad. Sci. USA. 2002; 99:9369–9373. [PubMed: 12077322]

26. Hwang I, Huang JF, Kishimoto H, Brunmark A, Peterson PA, Jackson MR, Surh CD, Cai Z, Sprent J. T cells can use either T cell receptor or CD28 receptors to absorb and internalize cell surface molecules derived from antigen-presenting cells. J. Exp. Med. 2000; 191:1137–1148. [PubMed: 10748232]

27. Sabzevari H, Kantor J, Jaigirdar A, Tagaya Y, Naramura M, Hodge J, Bernon J, Schlom J. Acquisition of CD80 (B7-1) by T cells. J. Immunol. 2001; 166:2505–2513. [PubMed: 11160311]

28. Hwang I, Sprent J. Role of the actin cytoskeleton in T cell absorption and internalization of ligands from APC. J. Immunol. 2001; 166:5099–5107. [PubMed: 11290791]

29. Tatari-Calderone Z, Semnani RT, Nutman TB, Schlom J, Sabzevari H. Acquisition of CD80 by human T cells at early stages of activation: functional involvement of CD80 acquisition in T cell to T cell interaction. J. Immunol. 2002; 169:6162–6169. [PubMed: 12444120]

30. Hudrisier D, Kessler B, Valitutti S, Horvath C, Cerottini JC, Luescher IF. The efficiency of antigen recognition by CD8+ CTL clones is determined by the frequency of serial TCR engagement. J. Immunol. 1998; 161:553–562. [PubMed: 9670927]

31. Kalergis AM, Boucheron N, Doucey MA, Palmieri E, Goyarts EC, Vegh Z, Luescher IF, Nathenson SG. Efficient T cell activation requires an optimal dwell-time of interaction between the TCR and the pMHC complex. Nat. Immunol. 2001; 2:229–234. [PubMed: 11224522]

32. Murtaza A, Kuchroo VK, Freeman GJ. Changes in the strength of co-stimulation through the B7/CD28 pathway alter functional T cell responses to altered peptide ligands. Int. Immunol. 1999; 11:407–416. [PubMed: 10221652]

33. Mostböck S, Vidal S, Schlom J, Sabzevari H. Enhanced levels of costimulation lead to reduced effector/memory CD8+ T cell functionality. J. Immunol. 2007; 179:3524–3534. [PubMed: 17785786]

34. Céfaï D, Schneider H, Matangkasombut O, Kang H, Brody J, Rudd CE. CD28 receptor endocytosis is targeted by mutations that disrupt phosphatidylinositol 3-kinase binding and costimulation. J. Immunol. 1998; 160:2223–2230. [PubMed: 9498761]

35. Itoh Y, Hemmer B, Martin R, Germain RN. Serial TCR engagement and down-modulation by peptide:MHC molecule ligands: relationship to the quality of individual TCR signaling events. J. Immunol. 1999; 162:2073–2080. [PubMed: 9973480]

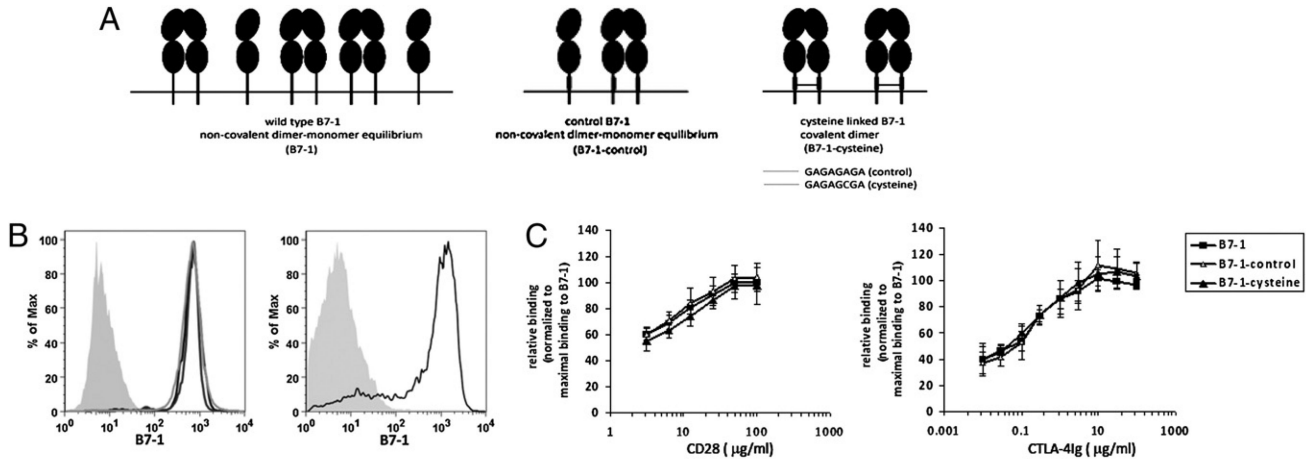

FIGURE 1.

Characterization of WT B7-1, B7-1–control, and B7-1–cysteine. A, Schematic representation of WT B7-1 or its mutants, engineered with an 8-aa residue linker sequence in the extracellular stalk region, with (B7-1–cysteine) or without (B7-1–control) cysteine. *B*, *Left panel*: Graphs showing the expression of WT B7-1 (black), B7-1–control (light gray), and B7-1–cysteine (dark gray) on CHO-IA^d cells. Shaded curve represents staining for B7-1 on untransfected CHO-IA^d cells. *Right panel*: Staining of B7-1 (black) on activated splenic dendritic cells; shaded curve represents the isotype control. *C*, Quantitative analysis of CD28Ig (*left graph*) and CTLA-4Ig (*right graph*) binding to WT B7-1, B7-1–control, and B7-1–cysteine expressing stable CHOIA^d transfectants. The relative binding at each concentration of CD28Ig or CTLA-4Ig was calculated as [fluorescence intensity B7-1_{mutant}/ maximal fluorescence intensity B7-1_{WT}] × 100. The results are the mean of four independent experiments; and the error bars represent the SE of the mean.

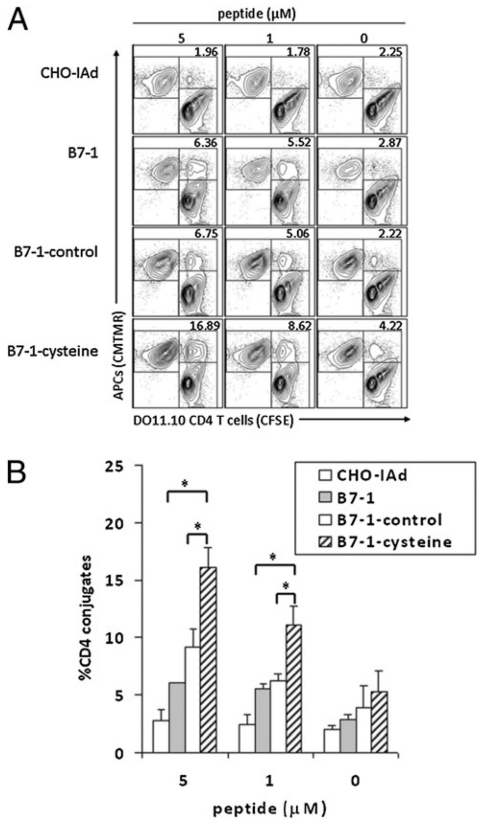

FIGURE 2.

Expression of obligate covalently linked B7-1 dimers increases CD28-mediated adhesion to T cells. A, CHO-IA^d cells expressing the covalently linked dimeric B7-1 show increased adhesion to T cells. CHO-IA^d cells untransfected (*top row*) or expressing WT B7-1 (*second row*), B7-1–control (*third row*), or B7-1–cysteine (*bottom row*) were pulsed with a titrated concentration of OVA peptide, labeled with CMTMR, and mixed with CFSE-labeled DO11.10 TCR Tg T cells. The CMTMR$^+$CFSE$^+$ CHO-IA^d–T cell conjugates were scored by flow cytometry. The numbers in the top right corner represent the percentage of T cells as T cell–APC conjugates. *B*, Quantification of CHO-IA^d–T cell conjugates as a percentage of total CD4 T cells. The results and error bars represent the means and SD from four independent experiments. *$p < 0.05$.

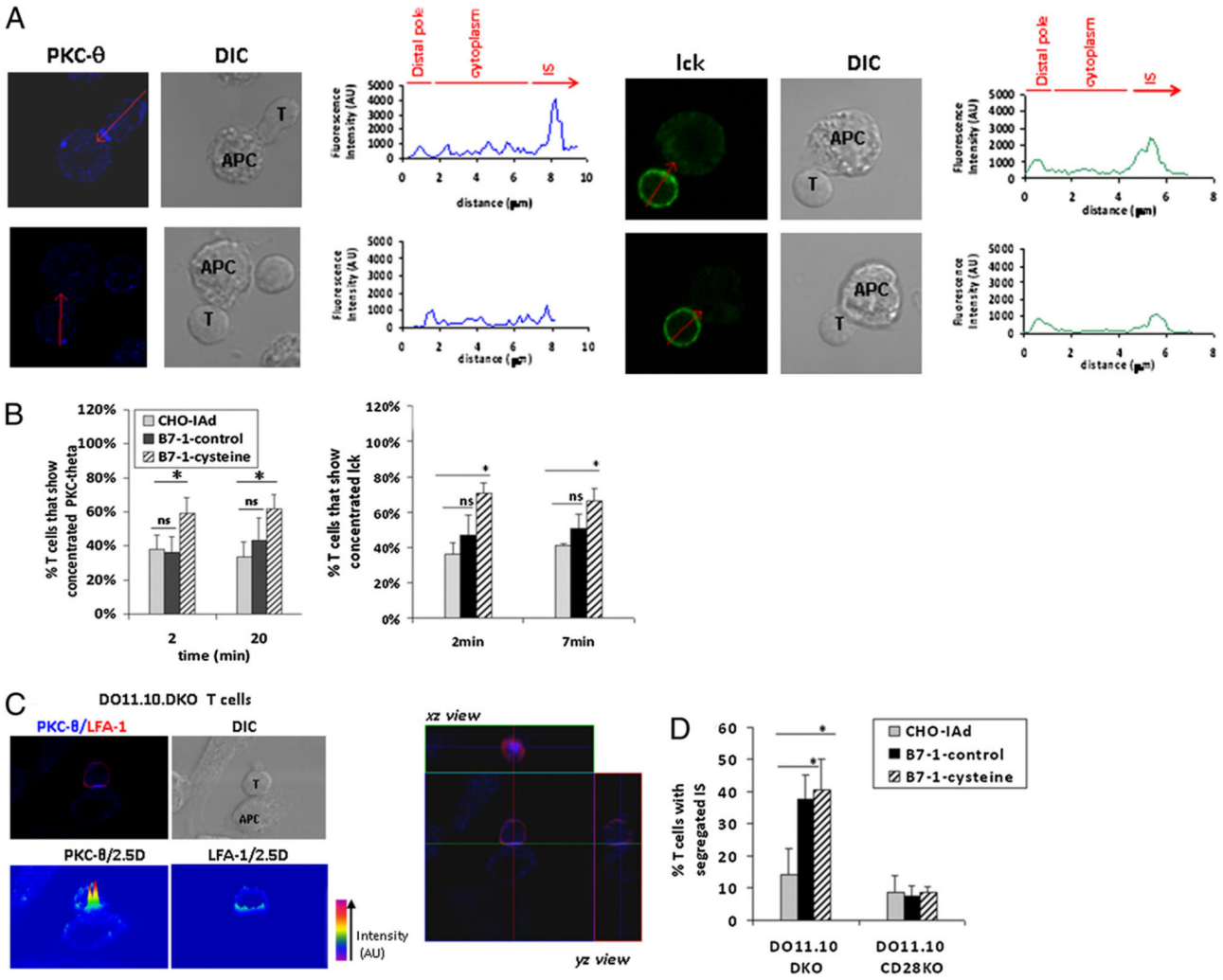

FIGURE 3.

Persistent concentration of PKC-θ and lck at the IS in the presence of covalently dimeric B7-1. A, Peptide-pulsed B7-1–transfected CHO-IA^d cells were fixed after mixing with DO11.10 CD4 T cells. The cells were stained for intracellular lck (green) and PKC-θ (blue). Arrow indicates the line of measurement of fluorescence intensity for PKC-θ or lck from distal area to contact area for the T cell–APC conjugates. The graphs show the fluorescence intensities of PKC-θ or lck along the marked arrow, extending from a region on the distal T cell membrane to a region on the T cell membrane in contact with APC. Fluorescence intensity was calculated as the area under the curve representing the IS or the distal membrane. The ratio of fluorescence intensity for the IS/fluorescence intensities for the distal membrane was used to calculate fold enrichment of the signaling molecules at the IS. T cell–APC conjugates that showed >2-fold enrichment of PKC-θ in the IS were scored as positive events. A representative image of T cells with >2-fold enrichment of PKC-θ (20 min) or lck (7 min) at the IS is shown in the respective upper panels, whereas the lower panels represent T cells that did not enrich PKC-θ or lck in the IS. *B*, Quantification of T cell conjugates with concentration of PKC-θ or lck at the IS. *Left graph*: Percentage of T cells showing concentration of PKC-θ in the IS at 2 and 20 min in the presence of CHO-IA^d (*n* =

167; 173), B7-1–control (*n* = 207; 153), or B7-1–cysteine (*n* = 190; 182). The results for PKC-θ represent the means and SE from four independent experiments. *Right graph*: Percentage of T cells showing >1.5-fold accumulation of lck in the IS at 2 and 7 min in the presence of CHO-IA^d (*n* = 97; 81), B7-1–control (*n* = 123; 138), or B7-1–cysteine (*n* = 111; 147). The results for lck represent the means and SE from three independent experiments. *C*, *Upper left*: Representative image of a mature IS characterized by PKC-θ and LFA-1 segregation in the IS of DO11.10.DKO T cells. *Bottom left*: Pseudo-colored 2.5D plot showing segregation of PKC-θ and LFA-1 in the IS. *Right*: Three-dimensional reconstruction of *z*-stacks of images showing the central localization of PKC-θ surrounded by peripheral LFA-1, characteristic of a mature IS. *D*, Quantification of T cell– APC conjugates that showed segregation of PKC-θ and LFA-1 in the IS. Thirty to 40 conjugates were visualized per group per experiment. The results are the mean and SE of three (for DO11.10.DKO) or two (DO11.10.CD28KO) independent experiments. *$p < 0.05$. ns, not significant.

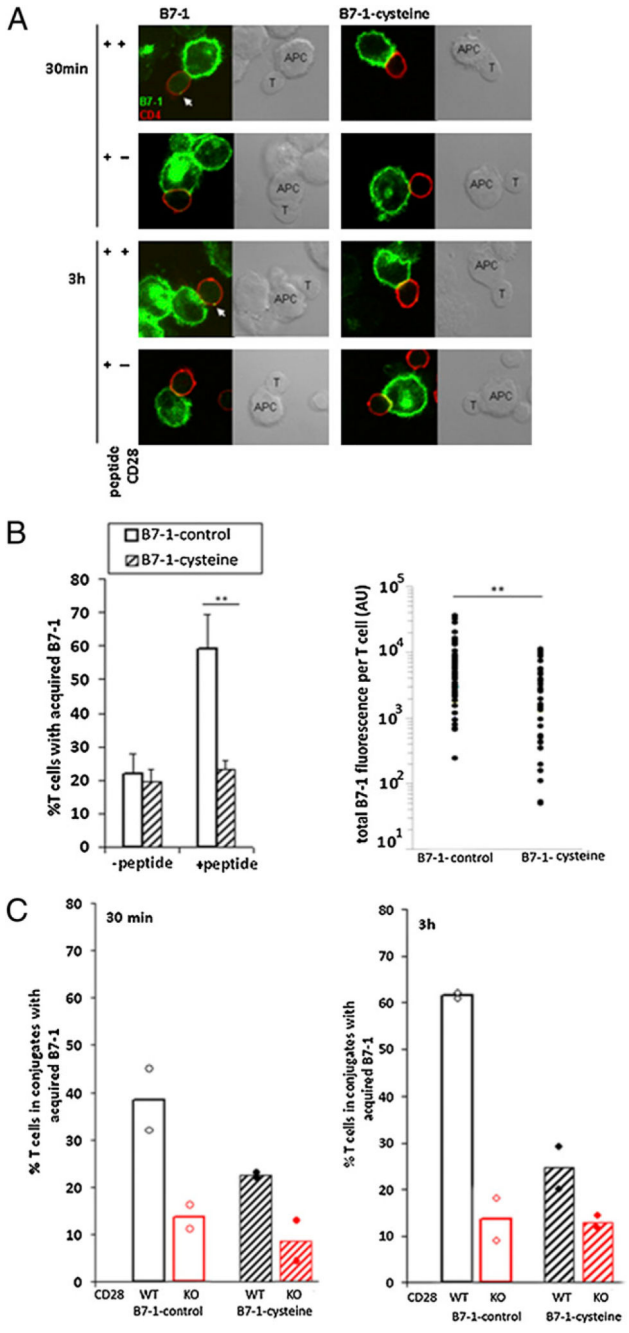

FIGURE 4.

Reduced acquisition of covalently dimeric B7-1 by T cells. A, Peptide-pulsed CHO-IA^{d}–B7-1 (*left panels*) or CHO-IA^{d}–B7-1-cysteine (*right panels*) cells were fixed at 30 min (*first and second rows*) or 3 h (*third and fourth rows*) after mixing with DO11.10 CD4 T (*first and third rows*) or DO11.10. CD28$^{-/-}$ CD4 T (*second and fourth rows*) cells. The cells were stained for intracellular B7-1 (green) and CD4 (red). T cells in T cell–APC conjugates that showed B7-1 fluorescence (intracellular or cell surface associated) greater than the threshold value obtained from T cells only were scored positive for the acquisition of B7-1. *B*, *Left panel*: Quantification of T cells in conjugates that show acquisition of B7-1 3 h after T cell–

APC conjugate formation in the absence or presence of OVA peptide. The results are mean and SD from six independent experiments. *Right panel*: Quantification of total B7-1 fluorescence per T cell. Each circle represents one T cell. Forty to 50 conjugates were visualized in each group. The results are representative of four independent experiments. $^{**}p$, 0.01. *C*, Quantification of T cells in conjugates that show acquisition of B7-1 at 30 min (*left graph*) or 3 h (*right graph*) after T cell–APC conjugate formation. The black bars indicate WT DO11.10 TCRTg CD4 T cells, whereas the red bars indicate DO11.10 TCR Tg CD28-deficient CD4 T cells. Forty to 50 conjugates were visualized in each group per experiment and is mean of two independent experiments; the circles represent individual experiments.

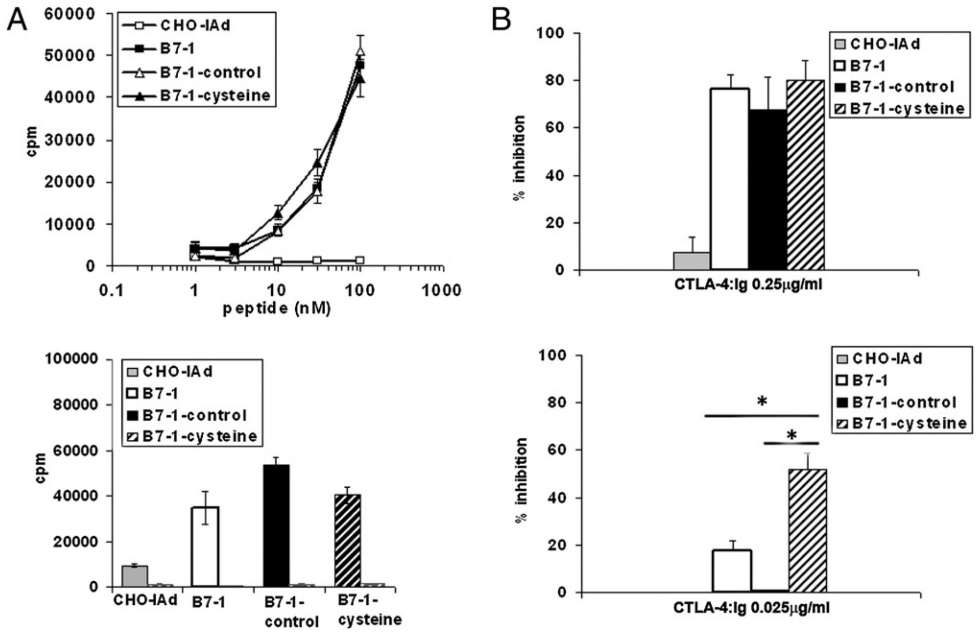

FIGURE 5.

B7-1–cysteine is less efficient in costimulating T cell proliferation. *A*, *Top panel*: DO11.10 $CD4^+$ T cells were stimulated with titrated concentrations of OVA peptide in the presence of CHO-IA^d cells that were untransfected or expressing WT B7-1, B7-1–control, or B7-1–cysteine as APCs for 48 h, after which the cultures were pulsed with 1 μCi of [^{3}H]thymidine for an additional 16 h. *Bottom panel*: $CD4^+$ T cells from DO11.10 B7 DKO (black bars) or CD28 KO (gray hatched bars) mice were stimulated with 30 nM OVA peptide in the presence of CHO-IA^d cells that were untransfected or expressing WT B7-1, B7-1–control, or B7-1–cysteine as APCs for 48 h and processed as described above. *B*, DO11.10 $CD4^+$ T cells were stimulated with OVA peptide (30 nM) in the presence of CHO-IA^d cells that were untransfected or expressing WT B7-1, B7-1–control, or B7-1–cysteine as APCs in the presence of 0.25 μg/ml (*top panel*) or 0.025 μg/ml (*bottom graph*) of CTLA-4–Ig for 48h, after which the cultures were pulsed with 1 μCi of [^{3}H]thymidine for an additional 16 h. Triplicate wells were harvested and counted. The percentage inhibition was calculated as {[(CPM without CTLA-4Ig) – (CPM with CTLA-4Ig)]/(CPM with CTLA-4Ig)} × 100. The results are the mean and SE of four independent experiments. *$p < 0.05$.

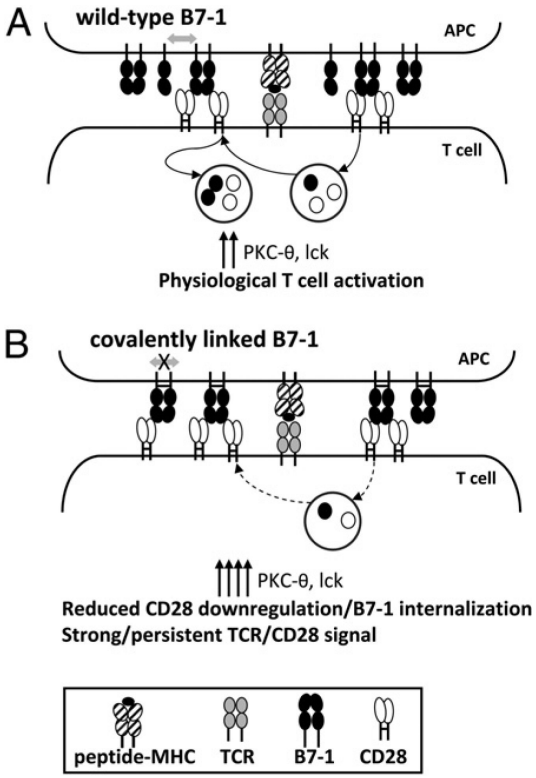

FIGURE 6.

Model for the interaction of B7-1 with CD28. A, Upon binding of noncovalent dimers of B7-1 to CD28, a fraction of CD28 is internalized, part of which is recycled back to the cell surface, whereas the remaining is targeted to lysosomes for degradation. Thus, the cell surface expression of CD28 is regulated by multiple mechanisms. The internalization of CD28 is also concomitant with the absorption of B7-1. Results of the present studies comparing noncovalent B7-1 dimers (B7-1–control) and covalently linked B7-1 dimers (B7-1–cysteine) suggest that this process of internalization of CD28 and acquisition of B7-1 may involve a key step of dissociation of noncovalent dimers of B7-1 (double-sided arrow). *B*, In the presence of a covalently linked dimeric form of B7-1, there is reduced acquisition of B7-1 and, presumably, reduced internalization of CD28. In the absence of dissociation of B7-1 dimers, signaling events, including IS localization of PKC-θ and lck, are increased and prolonged as the result of enhanced and/or sustained signaling via TCR/CD28.